^{13}C CP/MAS NMR Studies of Hemoprotein Models with and without an Axial Hindered Base: ^{13}C Shielding Tensors and Comparison with Hemoproteins and X-ray Structural Data

I. P. Gerothanassis,*,† M. Momenteau,*,‡ P. J. Barrie,§ C. G. Kalodimos,†,‡ and G. E. Hawkes||

Department of Chemistry, Section of Organic Chemistry and Biochemistry, University of Ioannina, Ioannina GR-451 10, Greece, Institut Curie, Section de Recherche, URA 1387 CNRS, Centre Universitaire, 91405 Orsay, France, Department of Chemistry, University College London, 20 Gordon Street, London WC1H OAJ, U.K., and Department of Chemistry, Queen Mary and Westfield College, Mile End Road, London E1 4NS, U.K.

Received July 7, 1995[⊗]

^{13}C cross-polarization magic-angle-spinning (CP/MAS) NMR spectra of several carbonmonoxide (93−99% ^{13}C enriched) hemoprotein models with 1,2-dimethylimidazole (1,2-diMeIm) and 1-methylimidazole (1-MeIm) as axial ligands are reported. This enables the ^{13}CO spinning sideband manifold to be measured and hence the principal components of the ^{13}CO chemical shift tensor to be obtained. Negative polar interactions in the binding pocket of the cap porphyrin model and inhibition of Fe→CO back-donation result in a reduction in shielding anisotropy; on the contrary, positive distal polar interactions result in an increase in the shielding anisotropy and asymmetry parameter in some models. It appears that the axial hindered base 1,2-dimethylimidazole has little direct effect on the local geometry at the CO site, despite higher rates of CO desorption being observed for such complexes. This suggests that the mechanism by which steric interactions are released for the 1,2-diMeIm complexes compared to 1-MeIm complexes does not involve a significant increase in bending of the Fe−C−O unit. The asymmetry of the shielding tensor of all the heme model compounds studied is smaller than that found for horse myoglobin and rabbit hemoglobin.

Introduction

The reversible binding of dioxygen and carbon monoxide has played a central role in studies of heme protein structure and function.[1−4] As a result, numerous encumbered iron(II) porphyrin models have been synthesized in an effort to elucidate the structural details of small ligand binding.[5] The steric bulk of certain axial ligands (e.g. 1,2-dimethylimidazole) bonded to synthetic iron(II) porphyrins provides model compounds of reduced O_2 and CO affinity, and models of the so-called tense state ("T" state) of hemoproteins.[6,7] Unfortunately, thus far there has only been one single-crystal X-ray structure determination on such a complex.[8] There has been much discussion on the mechanistic basis of the variation of affinity values in heme proteins and model compounds. This has focused on the nature of the axial ligand, distal steric effects, distal polar effects, and the enforced doming (conveniently measured by the difference in displacement of the four pyrrole nitrogen atoms and the 24-atom core) and ruffling (indicated by the displacements of the meso carbons relative to the porphyrin core mean plane) of the porphyrin skeleton.[1−5,9−12]

It is usually assumed that the Fe−C−O unit prefers a linear geometry, in order to maximize Fe d_π→CO π^* back-bonding, while the FeO_2 unit is strongly bent. Initial attention focused on this bent *vs* linear dichotomy and on the possibility that the CO binding is inhibited by steric interactions that impede a linear geometry.[13−15] More recently, emphasis has been given to polar interactions in the binding pocket.[16−20] Li and Spiro[17] have interpreted an inverse correlation between ν_{CO} and ν_{FeC} in terms

* Authors to whom correspondence should be addressed.
† University of Ioannina.
‡ Centre Universitaire.
§ University College London.
|| Queen Mary and Westfield College.
⊗ Abstract published in *Advance ACS Abstracts,* March 15, 1996.

(1) Dickerson, R. E.; Geis, I. *Hemoglobin, Structure, Function, Evolution and Pathology*; Benjamin Cummings: Menlo Park, CA, 1983; p 30.
(2) Perutz, M. F.; Fermi, G.; Luisi, B.; Shaanan, B.; Liddington, R. C. *Acc. Chem. Res.* **1987**, *20*, 309−321.
(3) Spiro, T. G. *Adv. Protein Chem.* **1985**, *37*, 111−159.
(4) Springer, B. A.; Sligar, S. G.; Olson, J. S.; Phillips, G. N., Jr. *Chem. Rev.* **1994**, *94*, 699−714.
(5) (a) Collman, J. P. *Acc. Chem. Res.* **1977**, *10*, 265−272. (b) Jones, R. D.; Summerville, D. A.; Basolo, F. *Chem. Rev.* **1979**, *79*, 139−179. (c) Traylor, T. G. *Acc. Chem. Res.* **1981**, *14*, 102−109. (d) Jameson, G. B.; Ibers, J. A. *Comments Inorg. Chem.* **1983**, *2*, 97−126. (e) Baldwin, J. E.; Perlmutter, P. *Top. Curr. Chem.* **1984**, *121*, 181−220. (f) Momenteau, M. *Pure Appl. Chem.* **1986**, *58*, 1493−1502. (g) Momenteau, M.; Reed, C. A. *Chem. Rev.* **1994**, *94*, 959−698. (h) Gerothanassis, I. P. *Prog. Nucl. Magn. Reson. Spectrosc.* **1994**, *26*, 239−292.
(6) Collman, J. P.; Reed, C. A. *J. Am. Chem. Soc.* **1973**, *95*, 2048−2049.
(7) Collman, J. P; Suslick, K. S. *Pure Appl. Chem.* **1978**, *50*, 951−961.
(8) Kim, K.; Fettinger, J.; Sessler, J. L.; Cyr, M.; Hugdahl, J.; Collman, J. P.; Ibers, J. A. *J. Am. Chem. Soc.* **1989**, *111*, 403−405.
(9) Collman, J. P.; Brauman, J. I.; Doxsee, K. M.; Halbert, T. R.; Suslick, K. S. *Proc. Natl. Acad. Sci. U.S.A.* **1978**, *75*, 564−568.
(10) Lavalette, D.; Tetreau, C.; Momenteau, M.; Mispelter, J.; Lhoste, J.-M.; Wuenschell, G. E.; Reed, C. *Laser Chem.* **1990**, *10*, 297−318.
(11) Tetreau, C.; Lavalette, D.; Momenteau, M.; Fischer, J.; Weiss, R. *J. Am. Chem. Soc.* **1994**, *116*, 11840−11848.
(12) Ray, G. B.; Li, X.-Y.; Ibers, J. A.; Sessler, J. L.; Spiro, T. G. *J. Am. Chem. Soc.* **1994**, *116*, 162−176.
(13) Collman, J. P.; Brauman, J. I.; Halbert, T. R.; Suslick, K. S. *Proc. Natl. Acad. Sci. U.S.A.* **1976,** *73*, 3333−3337.
(14) Collman, J. P.; Brauman, J. I.; Iverson, B. L.; Sessler, J. L.; Morris, R. M.; Gibson, Q. H. *J. Am. Chem. Soc.* **1983**, *105*, 3052−3064.
(15) Collman, J. P.; Brauman, J. I.; Collins, T. J.; Iverson, B. L.; Lang, G.; Pettman, R. B.; Sessler, J. L.; Walters, M. A. *J. Am. Chem. Soc.* **1983**, *105*, 3038−3052.
(16) Traylor, T. G.; Koga, N.; Deardurff, L. A. *J. Am. Chem. Soc.* **1985**, *107*, 6504−6510.
(17) Li, X.-Y.; Spiro, T. G. *J. Am. Chem. Soc.* **1988**, *110*, 6024−6033.
(18) Park, K. D.; Guo, K.; Adebodun, F.; Chiu, M. L.; Sligar, S. G.; Oldfield, E. *Biochemistry* **1991**, *30*, 2333−2347.
(19) Augspurger, J. D.; Dykstra, C. E.; Oldfield, E. *J. Am. Chem. Soc.* **1991**, *113*, 2447−2451.

0020-1669/96/1335-2674$12.00/0

of back-bond donation from the iron atom. These authors suggested that proton donors adjacent to the O atom of the bound ligand enhance the degree of back-bonding, thus resulting in an increase in the order of the Fe−C bond and a decrease in the order of the C−O bond. Oldfield and collaborators[18−20] emphasized the role of electrostatic influences on isotropic chemical shifts, quadrupole coupling constants, and vibrational frequencies in CO−heme proteins and free CO. They suggested that the electrical polarization and back-bonding concepts can provide a plausible molecular interpretation of both NMR and IR data of hemoproteins.

Recently we have developed the use of ^{13}C solid-state NMR spectroscopy as a probe of ^{13}CO environment in carbon monoxide hemoproteins and heme model compounds.[21,22] The ^{13}C shielding tensor of bound ^{13}CO may be obtained by simulation of spectra obtained using magic-angle spinning (MAS) at appropriate rates. The shielding tensor is expected to be a sensitive probe of any electronic differences at the ^{13}CO site between the complexes. In this paper, we report high-resolution ^{13}C solid-state NMR spectra on a number of hemoprotein model compounds both with and without an axial hindered base. Measurements were made on five different heme models (**A**−**E**) which either had 1-methylimidazole (**1-MeIm**) or 1,2-dimethylimidazole (**1,2-diMeIm**) in the axial position (see Figure 1). 1,2-diMeIm in the axial position of five-coordinate-iron complexes has significant steric interactions with the porphyrin ring, and thus may push the iron atom out of the porphyrin plane and induce an off-normal tilting of the imidazole, modeling the "T" state of deoxyhemoproteins.[6,7,23a−c] On the other hand, there are less unfavorable steric interactions with 1-MeIm and so the iron atom is expected to be closer to the porphyrin plane, modeling the high affinity "R" state of deoxyhemoproteins.[14c] Due to lack of knowledge of sufficient structural data, the object of this work was to identify any changes in the ^{13}C shielding tensors of bound ^{13}CO in six-coordinated-iron porphyrins as a result of varying the axial base in this fashion. Also, it was hoped that these further ^{13}C NMR measurements might in due course lead to a possible correlation of NMR data (e.g. the asymmetry parameter of the ^{13}C shielding tensor) with geometric information (e.g. the Fe−C−O bond angle derived from X-ray diffraction measurements).

Experimental Section

The iron (III) porphyrin superstructure complexes in the chloride form were synthesized and characterized by the methods described previously.[5,25−28] The complexes were shaken in either dichloromethane or toluene solution with an excess of aqueous sodium dithionite solution under argon. After separation of the two phases, the organic layer of

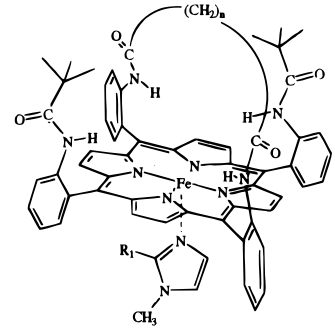

A (1-MeIm) : n = 10, R_1 = H
A (1,2-diMeIm) : n = 10, R_1 = CH_3
B (1-MeIm) : n = 6, R_1 = H
B (1,2-diMeIm) : n = 6, R_1 = CH_3

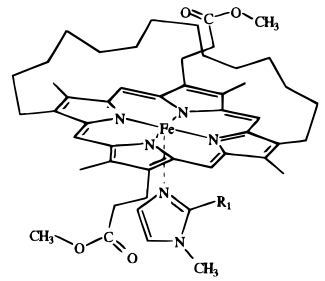

C (1-MeIm) : R_1 = H
C (1,2-diMeIm) : R_1 = CH_3

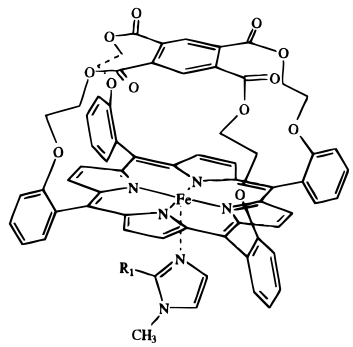

D (1-MeIm) : R_1 = H
D (1,2-diMeIm) : R_1 = CH_3

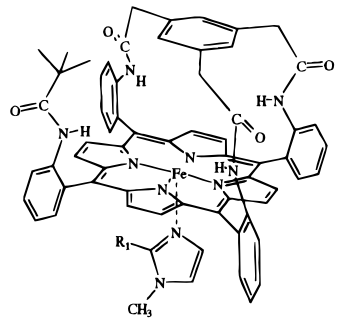

E (1-MeIm) : R_1 = H
E (1,2-diMeIm) : R_1 = CH_3

Figure 1. Schematic structures of heme model compounds studied in this work.

(20) Oldfield, E.; Guo, K.; Augspurger, J. D.; Dykstra, C. E. *J. Am. Chem. Soc.* **1991**, *113*, 7537−7541.
(21) Gerothanassis, I. P; Momenteau, M.; Hawkes, G. E; Barrie, P. J. *J. Am. Chem. Soc.* **1993**, *115*, 9796−9797.
(22) (a) Gerothanassis, I. P.; Barrie, P. J.; Momenteau, M.; Hawkes, G. E. *J. Am. Chem. Soc.* **1994**, *116*, 11944−11949. (b) Barrie, P. J.; Gerothanassis, I. P; Momenteau, M.; Hawkes, G. E. *J. Magn. Reson., B* **1995**, *108*, 185−188.
(23) (a) Jameson, G. B.; Molinaro, F. S.; Ibers, J. A.; Collman, J. P.; Brauman, J. I.; Rose, E.; Suslick, K. S. *J. Am. Chem. Soc.* **1978**, *100*, 6769−6770. (b) Jameson, G. B.; Molinaro, F. S.; Ibers, J. A.; Collman, J. P.; Brauman, J. I.; Rose, E.; Suslick, K. S. *J. Am. Chem. Soc.* **1980**, *102*, 3224−3237. (c) Momenteau, M.; Scheidt, W. R.; Eigenbrot, C. W.; Reed, C. A. *J. Am. Chem. Soc.* **1988**, *110*, 1207−1215.
(24) Abbreviations used : Mb, myoglobin ; Hb, hemoglobin ; 1-MeIm, 1-methylimidazole; 1,2-diMeIm, 1,2-dimethylimidazole; **A**, 5,15-[2,2'-(dodecanediamido)diphenyl]-α,α-10,20-bis(*o*-(pivaloylamino)phenyl)-porphyrin; **B**, 5,15-[2,2′-(octanediamido)diphenyl]-α,α-10,20-bis(*o*-(pivaloylamino)phenyl)porphyrin ; **C**, porphyrin bridged with C_{14} polymethylene "handle" in a cross configuration ; **D**, 5,10,15,20-[pyromellitoyltetrakis(*o*-(oxypropoxy)phenyl]porphyrin ; **E**, 5,10,15-(1,3,5-benzenetriyltriacetyl)-α,α,α-tris(*o*-aminophenyl)-α-20(*o*-pivalamidophenyl)porphyrin. Schematic structures of model porphyrins are shown in Figure 1.
(25) Momenteau, M.; Loock, B.; Tetreau, C.; Lavalette, D.; Croisy, A.; Schaeffer, C.; Huel, C.; Lhoste, J.-M. *J. Chem. Soc., Perkin Trans. 2* **1987**, 249−257.

reduced compounds was transferred under argon into a second vessel containing an excess of either 1-methylimidazole or 1,2-dimethylimidazole. The resulting powders obtained after evaporation of the organic solvent were then loaded into glass ampules, connected to a vacuum pump, and evacuated at room temperature for 24 h at a pressure of 10^{-4} Torr. ^{13}CO (93−99% enriched) under atmospheric pressure was then introduced to the samples to form the carbonylated derivative after diffusion of the ^{13}CO ligand. After 24 h, the glass ampules for the NMR work were sealed under reduced pressure. Schematic structures of the heme model compounds studied are shown in Figure 1. Independent synthesis and preparation of two of the complexes were also carried out in order to check for reproducibility of results.

The ^{13}C NMR spectra were obtained on the samples within the glass ampules at a frequency of 75.47 MHz using cross-polarization (CP), magic-angle spinning (MAS), and high-power proton decoupling[29,30] on a Bruker MSL-300 spectrometer. The interrupted decoupling technique, also known as nonquaternary suppression,[31] was used to remove signals from those ^{13}C nuclei with strong dipolar coupling to ^{1}H nuclei in order to reduce overlap of peaks arising from ^{13}CO with those arising from natural abundance ^{13}C in the porphyrin. For some samples, and myoglobin and hemoglobin in particular, the SELDOM pulse sequence (selectivity by destruction of magnetization)[32] was used to reduce further the problems of peaks overlap.

The spinning sideband intensities were simulated using an iterative fit programme based on the method of Herzfeld and Berger to obtain the principal components of the chemical shift tensor.[33,34] It is widely recognized that analysis of spinning sideband patterns from sites close to axial symmetry can be prone to quite large errors, and for this reason spectra were normally obtained at three different spinning rates (in the range 2.4−4.0 kHz). It was found that simultaneous fitting of the spectra significantly reduced the uncertainties in shielding tensor components. Calculated uncertainties represent 95% confidence limits, but do not take into account spectral noise. The resulting parameters are quoted using the convention that $\delta_{11} > \delta_{22} > \delta_{33}$, together with the anisotropy, $\Delta\sigma$, defined as $(\delta_{11} + \delta_{22})/2 - \delta_{33}$, and the asymmetry parameter, η, defined as $(\delta_{22} - \delta_{11})/(\delta_{33} - \delta_{iso})$ where the isotropic chemical shift, δ_{iso}, is $(\delta_{11} + \delta_{22} + \delta_{33})/3$.

Results and Discussion

Figure 2 shows typical ^{13}C spectra of the ^{13}CO complexes with heme model compounds, in this case samples **B(1-MeIm)** and **B(1,2-diMeIm)**, recorded using CP and nonquaternary suppression. The results of analyzing the spinning sideband intensities on all the complexes studied are shown in Table 1. It is found that there is normally no difference in isotropic chemical shift for the complexes studied when comparing the complexes with and without the axial hindered base. Further the variation in ^{13}CO isotropic chemical shift with porphyrin skeleton and organic superstructure is also small; the only complexes that fall significantly outside the range 204−205 ppm are samples **D(1-MeIm)** and **D(1,2-diMeIm)**, and this possibly reflects ring current effects from the distal aromatic ring rather than changes in the electronic structure at the ^{13}CO site.

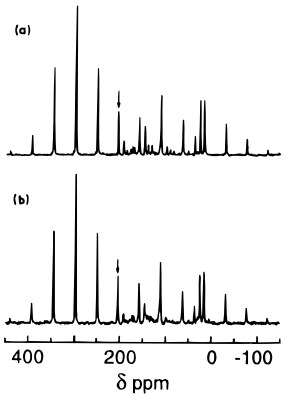

Figure 2. ^{13}C CP/MAS NMR spectra of ^{13}CO complexes with (a) **B-(1-MeIm)**, and (b) **B(1,2-diMeIm)**. The spectra were recorded with 40 μs interrupted decoupling (NQS) at a spinning speed of 3540 Hz using a contact time of 3 ms and a recycle delay of 2 s. The arrows denote the isotropic resonance.

While the isotropic chemical shifts are practically independent of the nature of both the axial ligand and the distal protecting chain, the three independent principal components, δ_{11}, δ_{22}, and δ_{33}, do show some variation. Thus in the axial hindered base complex **A(1,2-diMeIm)** (which has two pivalamido pickets and an amide handle linked in a cross-trans configuration) there is a shift to high frequency of δ_{11} and a shift to low frequency of δ_{22}, resulting in an increase in the value of the asymmetry parameter, η, relative to **A(1-MeIm)**. The changes in δ_{11} and δ_{22}, together with a small shift to low frequency of δ_{33}, also cause a small increase in the overall anisotropy, $\Delta\sigma$, relative to the unhindered complex. It should be emphasized that the ^{13}C chemical shift tensor is affected only by local factors influencing the shielding at the ^{13}C site such as electronic influences and magnetic anisotropy. Thus, increasing deviation from axial symmetry, as would be expected to be the case for decreasing Fe−C−O bond angle, will manifest itself as an increase in the value of the asymmetry parameter, η.

The X-ray structure of complex **A(1-MeIm)** shows that the Fe−C−O unit is both linear and normal to the mean porphyrin plane. All contacts between the terminal oxygen atom and the aliphatic bridging chain are longer than 4 Å[35] and the distance between the porphyrin mean plane and the aliphatic bridging chain is ≥ 8.4 Å (Table 2). This is significantly longer than distance measurements of the porphyrin mean plane and the organic superstructure in the pentacoordinated species.[23c] It is clear that the energetic cost associated with the modification of the organic superstructure accompanying CO binding is less than the energetic penalty which would accompany bending of the Fe−C−O unit. The NMR results indicate that the ^{13}C shielding tensor for this complex is axial ($\eta = 0$) within experimental error, as would be expected for a linear Fe−C−O unit.

As in the case of the **A** complexes, complex **B(1,2-diMeIm)** shows a small increase in the asymmetry parameter and a small increase in overall anisotropy compared to complex **B(1-MeIm)**. For complex **B(1-MeIm)** the small deviation from axial symmetry observed in the NMR analysis is consistent with X-ray structural data that shows a small bending of the Fe−C−O unit ($\theta = 178.3°$) without tilting (Table 2).[11] Moreover, the iron atom lies almost in the plane formed by the porphyrin nitrogens but is slightly displaced from the 24-atom core mean plane toward the 1-MeIm ligand.

For ^{13}CO in the **C** complexes there is a significant increase in the asymmetry of the shielding tensor relative to the complexes of **A** and **B**, which suggests that there may be increased bending of the Fe−C−O unit in these complexes. It is interesting to note that these samples also have higher rates

(26) (a) El-Kasmi, D.; Tetreau, C.; Lavalette, D.; Momenteau, M. *J. Chem. Soc., Perkin Trans. 2* **1993**, 1799−1803. (b) Leodiadis, L. Ph.D. Thesis, University "Paris-Sud", Orsay, 1991.
(27) Almog, J.; Baldwin, J. E.; Huff, J. R. *J. Am. Chem. Soc.* **1975**, *97*, 227−228.
(28) Collman, J. P.; Brauman, J. I.; Collins, T. J.; Iverson, B. L.; Lang, G.; Pettman, R. B.; Sessler, J.-L.; Walters, M. A. *J. Am. Chem. Soc.* **1983**, *105*, 3038−3052.
(29) Mehring, M. *High Resolution NMR Spectroscopy in Solids*; Springer-Verlag, Berlin, 1983.
(30) Fyfe, C. A. *Solid State NMR for Chemists*; (C.F.C. Press: Guelph, Ontario, 1983.
(31) Opella, S. J.; Frey, M. H. *J. Am. Chem. Soc.* **1979**, *101*, 5854−5855.
(32) Tekely, P.; Brondeau, J.; Elbayed, K.; Retournard, A.; Canet, D. *J. Magn. Reson.* **1988**, *80*, 509−516.
(33) Herzfeld, J.; Berger, A. E. *J. Chem. Phys.* **1980**, *73*, 6021−6030.
(34) Hawkes, G. E.; Sales, K. D.; Lian, L. Y.; Gobetto, R. *Proc. R. Soc. London A* **1989**, *424*, 93−111.
(35) Ricard, L.; Weiss, R.; Momenteau, M. *J. Chem. Soc., Chem. Commun.* **1986**, 818−820.

Table 1. Principal Components of the ^{13}C Chemical Shift Tensor[a] of Heme Compounds of Figure 1

compound[b]	δ_{iso}	δ_{11}	δ_{22}	δ_{33}	$\Delta\sigma$	η
A(1-MeIm)	205.0	358 ± 20	350 ± 19	-92 ± 2	446	0.03 ± 0.09
		354 ± 1[c]	354 ± 1[c]	-92 ± 1[c]	446[c]	0.00[c]
A(1,2-diMeIm)	205.7	372 ± 2	340 ± 3	-95 ± 1	451	0.11 ± 0.01
B(1-MeIm)	205.4	367 ± 3	345 ± 3	-96 ± 1	452	0.07 ± 0.01
B(1,2-diMeIm)	204.2	372 ± 3	343 ± 3	-102 ± 2	459	0.10 ± 0.01
C(1-MeIm)	205.0	385 ± 5	324 ± 3	-93 ± 2	447	0.20 ± 0.02
C(1,2-diMeIm)	205.0	385 ± 2	327 ± 1	-99 ± 2	455	0.19 ± 0.01
D(1-MeIm)	202.5	368 ± 14	331 ± 11	-92 ± 5	442	0.12 ± 0.06
D(1-MeIm)[d]	202.2	374 ± 12	320 ± 7	-87 ± 7	434	0.19 ± 0.05
D(1,2-diMeIm)	202.2	373 ± 1	326 ± 1	-93 ± 1	442	0.16 ± 0.01
D(1,2-diMeIm)[d]	202.5	373 ± 2	326 ± 2	-91 ± 2	441	0.16 ± 0.01
E(1-MeIm)	203.8	382 ± 2	327 ± 2	-97 ± 2	451	0.18 ± 0.01
E(1,2-diMeIm)	203.6	377 ± 3	332 ± 2	-98 ± 2	453	0.15 ± 0.01
Mb (crystals)[22,a]	205.5	394 ± 16	311 ± 12	-88 ± 7	440	0.28 ± 0.07
Mb (powder)[22,a]	205.5	390 ± 22	317 ± 18	-91 ± 5	445	0.25 ± 0.10
Hb[22,b]	205.0	390 ± 13	309 ± 7	-85 ± 8	435	0.28 ± 0.06

[a] Chemical shifts are given in ppm relative to TMS. See text for definitions of $\Delta\sigma$ and η. [b] Abbreviations are given in ref 24, and schematic structures are shown in Figure 1. [c] Results obtained by constraining to axial symmetry. [d] Results obtained from a second preparation and analysis.

Table 2. Structural Features and Rates of CO Desorption, k^{-CO}, for CO Binding with the Heme Compounds of Figure 1

compound[a]	C_{meso} mean displacement	shortest NH(amide)···O(CO) dist/Å	Fe···M dist/Å[b]	Fe−C dist/Å	Fe−C−O angle[c]/deg	$10^3 k^{-CO}/s^{-1}$ [c]
A(1-MeIm)	0.155	4.60	8.43	1.728	180(35)	2.7 (11)
A(1,2-diMeIm)						110 (11)
B(1-MeIm)	0.44	3.99	6.53	1.733	178.3(11)	8.2 (11)
B(1,2-diMeIm)						80 (11)
C(1-MeIm)						110 (26)
C(1,2-diMeIm)						560 (26)
D(1-MeIm)[d]	0.04		5.57	1.742	172.9(36)	50 (14)
D(1-MeIm)[d]	0.03		5.68	1.748	175.9(36)	
E(1-MeIm)						8.6 (14)
E(1,2-diMeIm)	0.53	3.76	3.99	1.768	172.5(8)	55.0 (14)

[a] Abbreviations are given in ref 24, and schematic structures are shown in Figure 1. [b] Fe···M is the distance between the centroid of distal cap or strap and the Fe atom; it defines the distal pocket size [c] Data taken from the references indicated in parentheses. [d] These are two independent Fe(C_2-cap)(1-MeIm)(CO) molecules within the asymmetric part of the unit cell.

of CO desorption, k^{-CO}, than the other model compounds in this study (Table 2). The most likely reason for any increased bending would be strong steric interactions with the distal protecting chain. The **C** complexes contain a C_{14} strap anchored to the pyrrole carbon positions of the porphyrin which leads to a smaller distance between the iron binding site and the distal protecting chain than in the complexes **A** and **B** (which have the chain anchored through an amide linkage to two opposite phenyl groups on the porphyrin), and it is possible that this leads to the increased asymmetry of the **C** complexes relative to **A** and **B**. However, no difference in the η values of **C(1-MeIm)** and **C(1,2-diMeIm)** is observed, although there is a small change in $\Delta\sigma$. Thus it appears that the local geometry at the ^{13}CO site and hence the steric interactions with the distal protecting chain are similar for complexes with the hindered and unhindered axial base.

For ^{13}CO in the **D** complexes, in which a benzene cap is attached by carboxylate links and a pair of methylene groups to the four hydroxyl groups of tetrakis(*o*-hydroxylphenyl)-porphyrin, asymmetric shielding tensors are also observed. The refined X-ray crystal structure of **D(1-MeIm)** shows the presence of two crystallographically independent porphyrin molecules, with the Fe−C−O groups distorted from linearity (172.9 and 175.9°, Table 2) and being tilted off the axis normal to the porphyrin (off-axis displacement for the carbon atoms being 0.17 and 0.12 Å, respectively).[36] These distortions result from short nonbonding interactions between the cap and the CO ligand although the center of the cap moves about 1.6−1.7 Å further away from the porphyrin, compared to H_2(C_2-Cap) and FeCl(C_2-Cap) X-ray structures,[37,38] and the cap is no longer parallel to the porphyrin plane. Interestingly, the porphyrin distortion is very small, presumably because of the constraint of the cap. Only a single ^{13}C isotropic resonance is observed for **D(1-MeIm)** which shows that the isotropic chemical shifts of the two conformations present are within 1 ppm of each other. Higher uncertainties in the principal components of the chemical shift tensor are obtained for **D(1-MeIm)** compared to the other complexes studied, and this probably reflects the presence of the two independent species in the unit cell with overlapping signals and slightly different shielding tensors. A second preparation and ^{13}C NMR analysis of **D(1-MeIm)** was also made; this gave slightly different shielding anisotropy results (though still within experimental error of each other). In contrast to the analysis of **D(1-MeIm)**, **D(1,2-diMeIm)** gives excellent agreement between experimental and simulated spectra, and a second independent preparation and analysis gave identical results for the two samples. The asymmetry parameters for both **D** complexes are consistent with some deviation from linearity of the Fe−C−O unit as is known from the crystal structure of **D(1-MeIm)**.

For the pocket superstructure **E** (which consists of a benzene cap attached to three out of four of the porphyrin phenyl substituents via *o*-amide linking groups and a fourth free pivalamido pocket) the shielding tensors were also found to be asymmetric. Kim *et al.*[8] have reported the X-ray crystal structure of the β-atropoisomer of **E(1,2-diMeIm)** (in which

(36) Kim, K.; Ibers, J. A. *J. Am. Chem. Soc.* **1991**, *113*, 6077−6081.
(37) Jameson, G. B.; Ibers, J. A. *J. Am. Chem. Soc.* **1980**, *102*, 2823−2831.
(38) Sabat, M.; Ibers, J. A. *J. Am. Chem. Soc.* **1982**, *104*, 3715−3721.

the fourth picket group is in the "down" position). The Fe−C−O bond angle was found to be 172.5° (Table 2) and the off-axis displacements of the C and O atoms are 0.18 and 0.38 Å, respectively. The modest distortion of the Fe−C−O unit is accompanied by considerable ruffling of the porphyrin periphery and significant shifting of the benzene "cap" away from the bound CO ligand. Moreover, the Fe atom is only 0.001 Å out of the 24-atom least squares plane toward the CO ligand. During our synthesis of **E(1,2-diMeIm)** we observed that both α- and β-atropoisomers exist in solution, with slow exchange between them. It is therefore likely that both forms exist in our powdered sample (unless the evaporation/crystallization procedure favors one particular form). In line with the crystal structure a deviation from axial symmetry is observed. No X-ray crystal structure is known for the model compound **E(1-MeIm)**, but analysis of EXAFS data recorded at 4 K in 1984 suggested that the Fe−C−O bond angle is 127 ± 4°.[39] However, more recent structural studies have called into question the interpretation of some early EXAFS results.[12] The asymmetry parameter for **E(1-MeIm)** is only slightly larger than that for **E(1,2-diMeIm)**, which indicates that any decrease in bond angle must be small and that the Fe−C−O moiety is far closer to linearity than that suggested by the early EXAFS study.

Comparison of the results for the **1-MeIm** and **1,2-diMeIm** complexes of all five porphyrins (**A**−**E**) surprisingly shows few significant differences. Shielding anisotropies of both **D(1-MeIm)** and **D(1,2-diMeIm)** are smaller than those of the other heme models particularly with that of the pocket model **E** although the X- ray structures of the two adducts show very similar FeCO bending. Presumably, this reflects different pocket polarity. In C_2-Cap there are no NH groups to provide positive polarity near the CO group and the lone pairs of the oxygen of the ester groups provide negative polarity.[12] Furthermore, the π electron cloud of the benzene ring is expected to inhibit back-donation from the Fe(II) d_π to the CO π* orbital due to the small distance between the center of the benzene ring and the CO oxygen (∼2.77 and 2.80 Å) for the two independent molecules in the cell). This argument is supported by the fact that the shielding anisotropies of both **D(1-MeIm)** and **D(1,2-diMeIm)** have values closer, compared to other heme model compounds of Table 1, to the experimental shielding anisotropy of free CO at 4.2 K ($\Delta\sigma$ ∼406 ± 30 ppm[40]) and the value for CO resulted from ab initio calculations ($\Delta\sigma$ ∼433.8 ppm[19]). Interestingly Ray *et al.*[12] showed that polar interactions with the superstructure of capped hemes, and not distortion due to steric hindrance, cause the large variations in ν_{CO} and ν_{FeC} observed for these compounds.

There may be a small increase in the asymmetry parameter, η, and shielding anisotropy, $\Delta\sigma$, for structures **A** and **B** on going from the **1-MeIm** to the **1,2-diMeIm** complexes. The hybrid model **A** has amide links, with the four N−H dipoles turned toward the iron atom. The distance of the secondary amide group of the chain and the CO ligand, (N)H···O(C), is 4.60 Å, thus providing an environment of positive polarity for the CO ligand. This polar interaction can be increased via the steric constraint of a short strap and the presence of an axially hindered base. Thus increase in the asymmetry parameter and shielding anisotropy might be expected for the **B(1-MeIm)** model, with an NH (amide)···O (C) distance of 3.99 Å,[41] compared to that of the model **A(1-MeIm)**. This is in agreement with the experimental results of Table 1. This distal polar effect and π-back-bonding concept is supported by the fact that the carbonyl shielding anisotropies of models **A** and **B** are significantly larger than those of the cap-model and free CO. In free CO, there is only one low-lying excited state of the proper symmetry to contribute to the paramagnetic shielding tensor component, $\sigma_\perp^{(p)}$, perpendicular to the CO internuclear axis. In the molecular orbital formalism, this excited state is formed from the ground state by promoting an electron from the 5σ to the 2π orbital. According to Gleeson and Vaughan[42] the 2π orbital would be destabilized through interaction with filled d orbitals, which are of intermediate energy between 5σ and 2π orbitals of CO. This excitation energy would thus be lowered and the paramagnetic contribution to $\sigma_\perp^{(p)}$, and thus shielding anisotropy, would be increased by the presence of the d orbitals. Further, π-back-bonding may increase the population on the CO π* orbitals[43] resulting in a high frequency shift of the $\sigma_\perp$ component[44] in agreement with the experimental results of Table 1. Interestingly Augspurger *et al.*[19] concluded that for the free CO an electric field oriented along the molecular axis polarizes charge density, and it primarily changes the perpendicular elements of the shielding tensor, thus resulting in an increase in shielding anisotropy. This is in agreement with our previous analysis on the effect of polar distal interactions on shielding anisotropies. The same polar effect has been suggested to account for the back-bonding trends seen in resonance Raman studies for a series of strapped porphyrins by Yu *et al.*[45] and hybrid models by Desbois *et al.*[46]

Contrary to models **A** and **B** there is no effect of axial base on the asymmetry parameter for the complexes **C** and **D**, even though changing to a hindered base is known to increase CO desorption rates (Table 2). Thus it appears that the axial hindered base has little direct effect on the ^{13}CO environment, but exerts its influence through distortion of the porphyrin skeleton and modification of the organic superstructure. This view is supported by the X-ray crystal structure of the CO complexes of **E(1,2-diMeIm)** which shows modest distortion of the carbonyl subunit, but considerable ruffling of the porphyrin periphery.[8]

The asymmetry of the shielding tensor of all the heme model compounds studied is significantly smaller than that found for horse myoglobin and rabbit hemoglobin (see Table 1).[22,47] For Mb^{13}CO the increase in asymmetry may be attributed to an interaction in the A_3 substrate, which was found to be the major conformer in the samples used for ^{13}C CP MAS NMR measurements,[22a] of the N_ϵ lone pair of the distal histidine with

(39) Powers, L.; Sessler, J. L.; Woolery, G. L; Chance, B. *Biochemistry* **1984**, *23*, 5519−5523.

(40) Duncan, T. M.; Yates, J. T. Jr.; Vaughan, R. W. *J. Chem. Phys.* **1980**, *73*, 975−985. The static principal component values and shielding anisotropy were computed by assuming the chemical shift anisotropy of $\Delta\sigma$ = 365 ppm at 4.2 K (from Gibson, A. A. V.; Scott, T. A.; Fukushima, E. *J. Magn.Reson.* **1977**, *27*, 29) and an isotropic shift of 181.3 ppm. The anisotropy is believed to be averaged by rapid vibrational modes at 4.2 K.

(41) The crystal structure of the **B(1-MeIm)** model indicates that one of the amide groups of the chain is rotated by 90°.[35]

(42) Gleeson, J. W.; Vaughan, R. W. *J. Chem. Phys.* **1983**, *78*, 5384−5392.

(43) Brown, D. A.; Rawlinson, R. M. *J. Chem. Soc. A* **1969**, 1530−1534, 1534−1537.

(44) Huang, Y.; Gilson, D. F. R.; Butler, I. S.; Morin, F. G. *Inorg. Chem.* **1992**, *31*, 322−323.

(45) Yu, N.-T.; Kerr, E. A.; Ward, B.; Chang, C. K. *Biochemistry* **1983**, *22*, 4534−4550.

(46) Desbois, A.; Momenteau, M.; Lutz, M. *Inorg. Chem.* **1989**, *28*, 825−835.

(47) ^{13}C NMR spectra of Hb^{13}CO in solution demonstrate the presence of two ^{13}CO resonances, separated by 2 ppm, corresponding to distinct ^{13}CO environments in the α and β subunits (see: Moon, R. B.; Richards, J. H. *J. Am. Chem. Soc.* **1972**, *94*, 5093−5095 and Matwiyoff, N. A.; Vergamini, P. J.; Needham, T. E.; Gregg, C. T.; Volpe, J. A.; Caughey, W. S. *J. Am. Chem. Soc.* **1973**, *95*, 4429−4431). These different conformers, which may have different anisotropies, are not resolved in our ^{13}C solid-state spectra; therefore, the chemical shift tensor components reported in Table 1 have been analyzed in terms of a single "average" site.[22b]

the CO π^* orbital.[12,48] Such a hypothesis is supported from neutron diffraction structure analysis[49] which showed that there was no hydrogen bond between CO and the distal histidine residue and that the N_ϵ atom is not deuterated. Apparently the imidazole proton resides on N_δ. This means that the lone pair, rather than a hydrogen bond donor, faces the bound CO. In principle, we would expect there to be a correlation between the asymmetry parameter, η, and the Fe−C−O bond angle. However, there are only a limited number of accurate Fe−C−O bond angles known in the literature for this type of complexes, and the uncertainties in measurements of η close to axial symmetry can be quite large. The bond angles known for the complexes studied are given in Table 2. It can be seen that the CO complexes of **A(1-MeIm)** and **B(1-MeIm)**, with Fe−C−O bond angles very close to linearity, have asymmetry parameters less than 0.10, while the CO complexes of **D(1-MeIm)** and **E-(1,2-diMeIm)**, which show a greater deviation from linearity, have asymmetry parameters of about 0.15. Given that the measured asymmetry parameter for MbCO and HbCO is 0.28, this suggests that the Fe−C−O bond angle must be significantly less than 172.5°; a linear correlation of Fe−C−O bond angle against η for the above complexes would imply an Fe−C−O bond angle in the range 160−169°. This is consistent with the most recent X-ray structural measurement on MbCO which showed a Fe−C−O bond angle of 160° at 1.5 Å resolution.[50] This agrees also with recent IR studies[12,51,52] which preclude Fe−C−O angles as small as 120−140° values reported from early determinations of MbCO crystal structures containing disordered CO.[49,53]

Acknowledgment. We are grateful for financial support from NATO (Collaborative Research Grant No. 921420), the Secretariat General pour la Recherche et la Technologie (Coopération Scientifique Franco-Hellénique), and the Centre National de la Recherche Scientifique, France. The NMR spectra were obtained on the ULIRS solid-state NMR facility at UCL. We wish to thank Mr. J. Cowley (QMW) for his expertise in producing sealed glass ampules suitable for MAS work.

IC950830R

(48) Makinen, M. W.; Houtchens, R. A.; Caughey, W. S. *Proc. Natl. Acad. Sci. U.S.A.* **1979**, *76*, 6042−6046.
(49) Cheng, X.; Schoenborn, B. P. *J. Mol. Biol.* **1991**, *220*, 381−399.
(50) Schlichting, I.; Berendzen, J.; Philips Jr., G. N.; Sweet, R. M. *Nature* **1994**, *371*, 808−812.
(51) Ivanov, D.; Sage, T.; Keim, M.; Powell, J. R.; Asher, S. A.; Champion, P. M. *J. Am. Chem. Soc.* **1994,** *116*, 4139−4140.
(52) Li, T.; Quillin, M. L.; Phillips, G. N. Jr.; Olson, J. S. *Biochemistry* **1994**, *33*, 1433−1446.
(53) Kuriyan, J.; Wilz, S.; Karplus, M.; Petsko, G. A. *J. Mol. Biol.* **1986**, *192*, 133−154.